A high coverage Mesolithic aurochs genome and effective leveraging of ancient cattle genomes using whole genome imputation.

Jolijn A.M Erven[1,2], Amelie Scheu[2,3], Marta Pereira Verdugo[2], Lara Cassidy[2], Ningbo Chen[4], Birgit Gehlen[5], Martin Street[6], Ole Madsen[7], Victoria E Mullin[2*]

*corresponding author: mullinve@tcd.ie

Author Affiliations

1. Groningen Institute of Archaeology, University of Groningen, Groningen, Netherlands
2. Smurfit Institute of Genetics, Trinity College Dublin, Dublin D02 PN40, Ireland
3. Palaeogenetics Group, Institute of Organismic and Molecular Evolution (iOME), Johannes Gutenberg-University Mainz, 55099 Mainz, Germany
4.Key Laboratory of Animal Genetics, Breeding and Reproduction of Shaanxi Province, College of Animal Science and Technology, Northwest A&F University, Yangling 712100, China
5. Institute for Prehistory and Protohistory, University of Cologne, Weyertal 125, 50931, Cologne, Germany
6. MONREPOS, Archaeological Research Centre and Museum for Human Behavioural Evolution,Schloss Monrepos, D - 56567 Neuwied, Germany
7.Animal Breeding and Genomics, Wageningen University and Research, Wageningen, Netherlands

Abstract

Ancient genomic analyses are often restricted to utilising pseudo-haploid data due to low genome coverage. Leveraging low coverage data by imputation to calculate phased diploid genotypes that enable haplotype-based interrogation and SNP calling at unsequenced positions is highly desirable. This has not been investigated for ancient cattle genomes despite these being compelling subjects for archaeological, evolutionary and economic reasons. Here we test this approach by sequencing a Mesolithic European aurochs (18.49x; 9852-9376 calBC), an Early Medieval European cow (18.69x; 427-580 calAD), and combine these with published individuals; two ancient and three modern. We downsample these genomes (0.25x, 0.5x, 1.0x, 2.0x) and impute diploid genotypes, utilising a reference panel of 171 published modern cattle genomes that we curated for 21.7 million (Mn) phased single-nucleotide

polymorphisms (SNPs). We recover high densities of correct calls with an accuracy of >99.1% at variant sites for the lowest downsample depth of 0.25x, increasing to >99.5% for 2.0x (transversions only, minor allele frequency (MAF) ≥2.5%). The recovery of SNPs correlates with coverage, on average 58% of sites are recovered for 0.25x increasing to 87% for 2.0x, utilising an average of 3.5 million (Mn) transversions (MAF ≥2.5%), even in the aurochs which is temporally and morphologically distinct from the reference panel. Our imputed genomes behave similarly to directly called data in allele-frequency-based analyses; for example consistently identifying runs of homozygosity >2mb, including a long homozygous region in the Mesolithic European aurochs.

Introduction

Cattle are ubiquitous and have been a significant economic and cultural resource for millennia. Taurine cattle (*Bos taurus*) were initially domesticated from the now extinct aurochs (*Bos primigenius*) *circa* 10,500 years BP in southwest Asia (Vigne et al., 2017), with additional introgression from local wild populations in Africa, Europe and the Levant (Park et al., 2015; Verdugo et al., 2019). Indicine cattle (*Bos indicus*) are adapted to warmer climates and descend from the recruitment of a divergent aurochs population (*Bos namadicus*), likely in the Indus Valley region ~8,000 years BP (Patel & Meadow, 2017). Cattle genetic variation is highly studied but their evolutionary history is incompletely understood, with ancient genome investigation required to uncover key processes in prehistory. For example, human-mediated movement of indicine cattle resulted in widespread admixture between taurine and indicine cattle in southwest Asia at least 4,200 years BP, resulting in hybrid cattle which persist in the region today (Verdugo et al., 2019). However, as archaeological remains are usually low in overall DNA concentration and endogenous DNA content, ancient genomes are typically low coverage (<5x) (Daly et al., 2018; Frantz et al., 2019; Librado et al., 2021; Verdugo et al., 2019), preventing confident diploid calling and limiting analyses to pseudo-haploid data, the sampling of one allele per variant site.

Genotype imputation - the statistical inference of unobserved genotypes by utilisting reference panels of haplotypes - is now a widely used methodological approach in ancient human genomics (Cassidy et al., 2020; Gamba et al., 2014; Martiniano et al., 2017). Specifically the development of GLIMPSE, a tool created for imputation from low-coverage genomes (Rubinacci et al., 2021), has enabled efficient imputation of large ancient human datasets (Clemente et al., 2021; Hui et al., 2020; Rohland et al., 2022; Sousa da Mota et al., 2023)ancient pigs (Erven et al., 2022). Imputing low coverage ancient genomes enables inferences of genome-wide diploid genotypes, diversifying analyses to include haplotype-focused or genealogical methods; *e.g*. inference of autozygosity within, and identity by descent between genomes. While genotype imputation is regularly used in modern livestock genetics, including cattle, (Hayes & Daetwyler, 2019), the efficacy of imputation has not been explored in ancient cattle.

In order to explore the imputation and subsequent analyses of ancient *Bos* we sequenced high coverage genomes (>18x) of a Mesolithic German female aurochs and an Early Middle Ages Dutch cow. We combine these with two previously published high (>13x) coverage ancient genomes (a Neolithic Anatolian domesticate and a Medieval taurine x indicine hybrid from Iraq (Verdugo et al., 2019) and three modern cattle genomes of different ancestries (European *Bos taurus*, African *Bos taurus* and *Bos indicus*). A reference panel of 171 publicly available modern cattle genomes, composed of *Bos taurus* and *Bos indicus*, was aligned and curated for 21.7 million (Mn) single-nucleotide polymorphisms (SNPs). By downsampling the test individuals, imputing with GLIMPSE and comparing analyses from direct genotype calls we establish that this approach is both feasible and desirable for leveraging low coverage ancient genome sequences, even for the extinct European aurochs.

Results & Discussion

The first high coverage ancient European aurochs and domestic cattle genomes.

Two ancient cattle genomes have been published with sequencing density sufficient for accurate genome-wide genotype calls; a Neolithic Turkish sample (Sub1; 6221-6024 calBC, 13.85x) and a Medieval taurus-indicus hybrid sample from Iraq (Bes2; 1295-1398 calAD, 13.8x) (Verdugo et al., 2019). Here we additionally report the first ancient European domesticate to high coverage, a 18.69x Early Middle Ages Dutch female (Win1) from Winsum-Bruggeburen (424-569 calAD). We also report the first high coverage Mesolithic female European aurochs (Bed3; 9852-9376 calBC) 18.49x genome excavated in Bedburg-Königshoven, Germany (Table SI 1). When we apply standard allele-frequency-based analysis methods (Figure 1) Win1 clusters with modern southern and central European cattle and Bed3 falls close to a published younger Mesolithic British aurochs (CPC98 - 5746-5484 calBC (Park et al., 2015). As expected, Sub1 clusters with other Neolithic Anatolian samples, while the position of Bes2 confers its hybrid ancestry (Verdugo et al., 2019).

Ancient cattle genomes impute non-rare alleles to high accuracy.

We assembled, aligned and variant called, a phased reference panel of 171 published high coverage (>7.6x) modern cattle genomes of varying ancestries, and with a geographical distribution including Europe, Africa and Asia (Method Section–Variant Discovery; Figure 1, Table SI 2). Variants called with Graphtyper were curated with stringent filters (Methods-Variant Discovery), resulting in 21,656,052 high-confidence SNPs, including 6,521,311 transversions (Table SI 2).

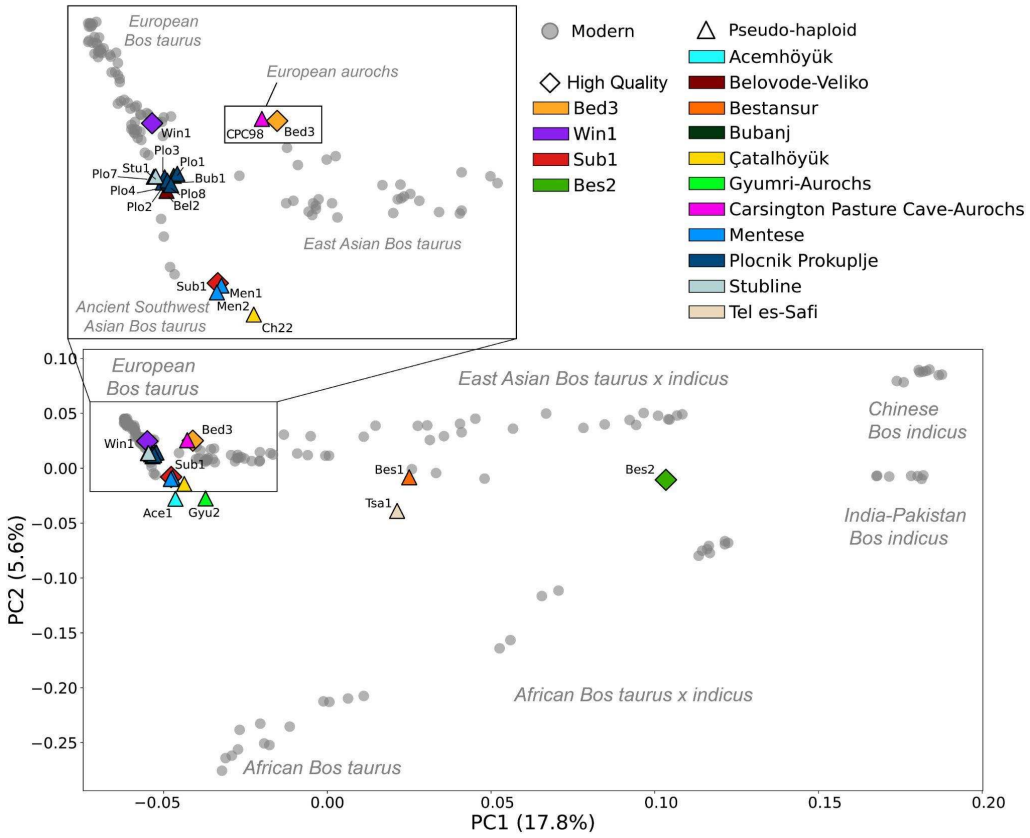

Figure 1) Principal Components analysis of ancient cattle. Bed3 and Win1 along with previously published ancient cattle are projected onto modern cattle diversity shown in grey circles. The four test ancient genomes are represented by diploid calls denoted as diamonds and coloured by sample, while previously published low coverage ancient samples are pseudo-haploid and are denoted by triangles and coloured by site (Table SI 1). Bed3 clusters with the previously published British Aurochs CPC98, while Win1 clusters with modern Southern European *Bos taurus*.

The four ancient *Bos* along with three previously published modern genomes (European *Bos taurus,* African *Bos taurus* and *Bos indicus*) were successfully imputed from a range of downsampled coverages (0.25x, 0.5x, 1x, 2x) using the newly created reference panel (Method section–Variant Discovery). Imputation accuracy, the concordance between imputed genotypes (GP ≥0.99 and INFO ≥0.99) and high quality validation genotypes for the high coverage genomes was calculated for heterozygous and homozygous alternative sites via PICARD GenotypeConcordance (“Picard Toolkit,” 2019); this accuracy is relatively stable over the different genome coverages when tested with transversions only (Figure 2a; Table SI 3).

126 However, rare alleles are affected more by a reduction in genome coverage (Figure 2a).
127 Notably, this trend is also present when all sites (transitions and transversions) are considered
128 (Figure SI 1; Table SI 4).

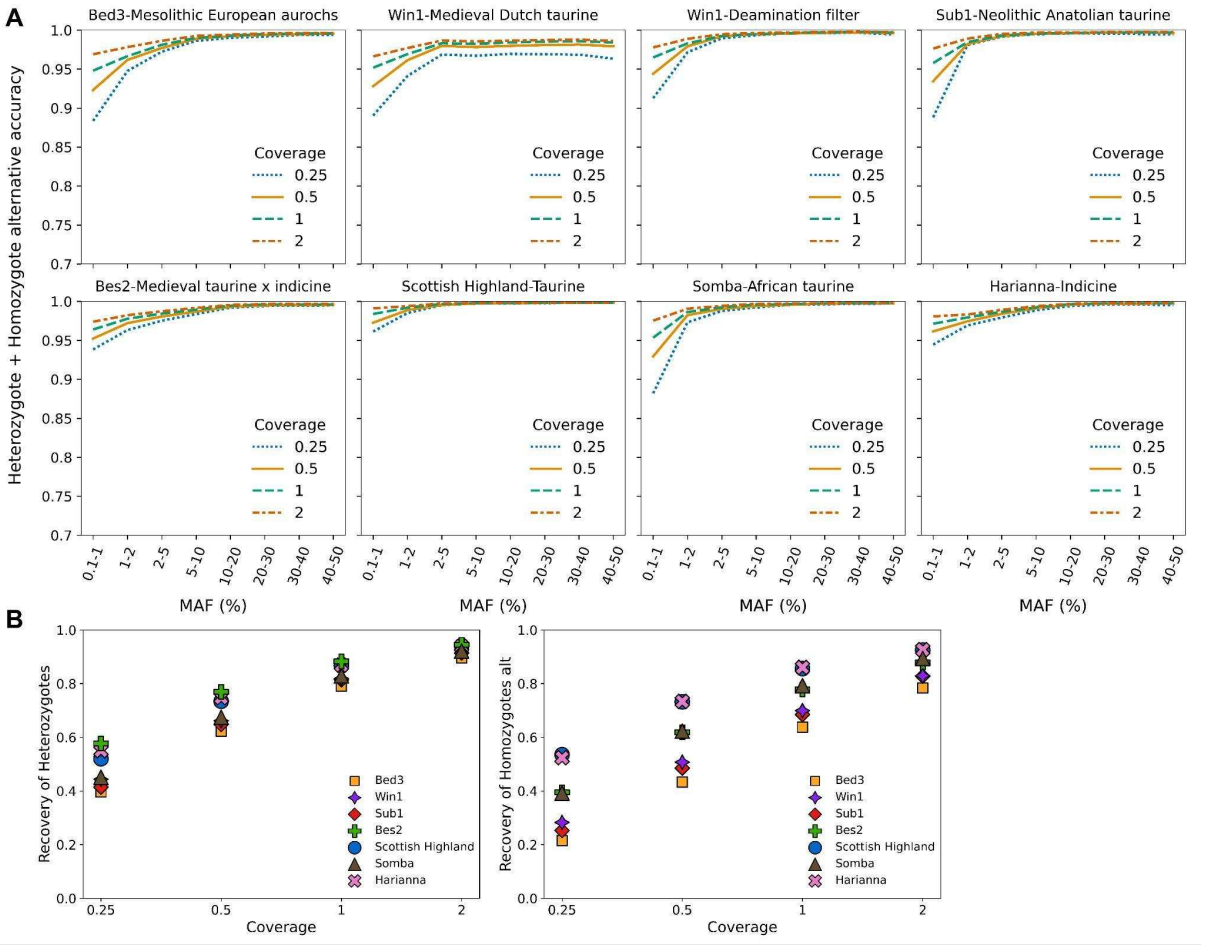

129

130 **Figure 2) A**) Accuracy of imputation of heterozygous and homozygous alternative sites at different
131 minor allele frequency (MAF) bins and different downsampled coverages, transversions only and with
132 a GP and INFO filter ≥0.99. Downsampled coverage is denoted by line style and colour. An additional
133 graph is included for Win1 to demonstrate the positive effect on the accuracy of a deamination filter
134 prior to imputation. **B**) Recovery rate of heterozygotes and homozygotes alternative for the different
135 downsampled coverages (MAF ≥ 2.5%, transversions only, GP ≥0.99 and INFO ≥0.99), with samples
136 denoted by shape and colour.
137
138 Across the coverage range, more common alleles have high accuracy, but this reduces for
139 rarer alleles, with a marked falling off at minor allele frequency (MAF) <5% (Figure 2a). The
140 lowest rare allele accuracies are observed in the Mesolithic European aurochs, Neolithic

Anatolian domestic and modern African taurine samples. This reduction in accuracy is likely due to the underrepresentation of these ancestries in the reference panel (Method section–Variant Discovery; Table SI 2). A similar trend is also observed in non-European ancient humans (Cassidy et al., 2016; Gamba et al., 2014; Martiniano et al., 2017; Sousa da Mota et al., 2023). Additionally, heterozygous sites have a higher accuracy than homozygous alternative sites at more common (MAF >10%) alleles (Table SI 3).

When we consider transversions with a MAF minimum threshold of 2.5%, the lowest accuracy is observed at the lowest downsample coverage of 0.25x (Win1 96.8%, Bed3 99.08%, Bes2 99.1%, Sub1 99.52%) (Table SI 5). It is interesting that, despite the highest temporal (>10,000 yr) distance from the contemporary reference panel, the aurochs Bed3 performs well, for example better than the more recent European domesticate Win1. This implies that the modern reference imputation panel contains a substantial degree of segregating European wild haplotype variants, presumably due to introgressions over the thousands of years when wild and herded animals cohabited on the continent (Park et al., 2015; Verdugo et al., 2019). A similar pattern has also been observed in the imputation of ancient humans, when Indigenous Americans are accurately imputed despite the lack of unadmixed Indigenous American genomes in a reference panel (Cassidy et al., 2016; Gamba et al., 2014; Martiniano et al., 2017; Sousa da Mota et al., 2023). In our data, despite its relatively young provenance, Win1 has an elevated damage profile at CpG sites in the first and last 30bp of the sequencing reads (Figure SI 2). When we filter potential deamination signals in this genome prior to imputation (Figure 2a, Figure SI 3) we demonstrate an improvement in imputation accuracy at each downsampled coverage; at the lowest depth of 0.25x accuracy increases from 96.8% to 99.6% for transversions with MAF ≥ 2.5%.

Our ancient samples are of diverse provenance. In addition to the European wild and northwest European domestic genomes, we also successfully impute an Anatolian Neolithic *Bos taurus* proximal to the origins of cattle in Southwest Asia and a *Bos indicus x Bos taurus*

hybrid from Iraq. These results suggest a wide potential for accurate genotype imputation of ancient cattle.

Ancient imputation achieves genome-wide genotype recovery

Variation is demonstrated in the proportion of genotypes which are recovered, with a clear positive trend between genome coverage and site recovery rate (Figure 2B & Table SI 3-5). The average recovery rate of heterozygote, homozygote alternative and homozygote reference sites for the ancient genomes at a depth of 2x was 87.3% (3.0 Mn sites), while a rate of 58.0% (2.1 Mn sites) was achieved at a depth of 0.25x (MAF ≥2.5%, transversions only, GP ≥0.99 and INFO ≥0.99) (Table SI 5). Across the downsampled coverages the recovery rate for heterozygote and homozygote alternative sites was higher in the modern genomes (39.2%-92.7% at 0.25x-2x coverage) than the ancients (30.6%-91.2%) (MAF ≥2.5%, transversions only) (Figure 2B). Additionally, when partitioning the data by MAF bins the recovery rate differs between heterozygotes and homozygotes alternative to the reference genome, where heterozygotes have a higher rate with more common alleles than homozygotes alternative, a trend which reverses with rare alleles, mirroring the accuracy results (Table SI 3).

Imputed genomes allow accurate analysis outcomes

We conducted unsupervised frequency-based analyses which are commonly used in ancient population genomics (*i.e.* PCA, ADMIXTURE) demonstrating a positive trend between accuracy and increasing downsample coverage (Figure SI 5-9). Here we report analyses utilising the 0.5x downsample imputation (Figure 3A). These analyses were accurate; the projection PCA demonstrates clustering between each high-quality and imputed replicate with the greatest eigenvector difference observed for the modern African taurine individual (Somba) across PC2 (Figure 3). ADMIXTURE analysis also estimated similar spectra of ancestral component profiles between imputed and high-quality genotypes (Figure SI 8-9).

196 This successful replication included analysis of the most temporally distant sample, the
197 ~11,500 yr old Mesolithic European aurochs (Bed3).

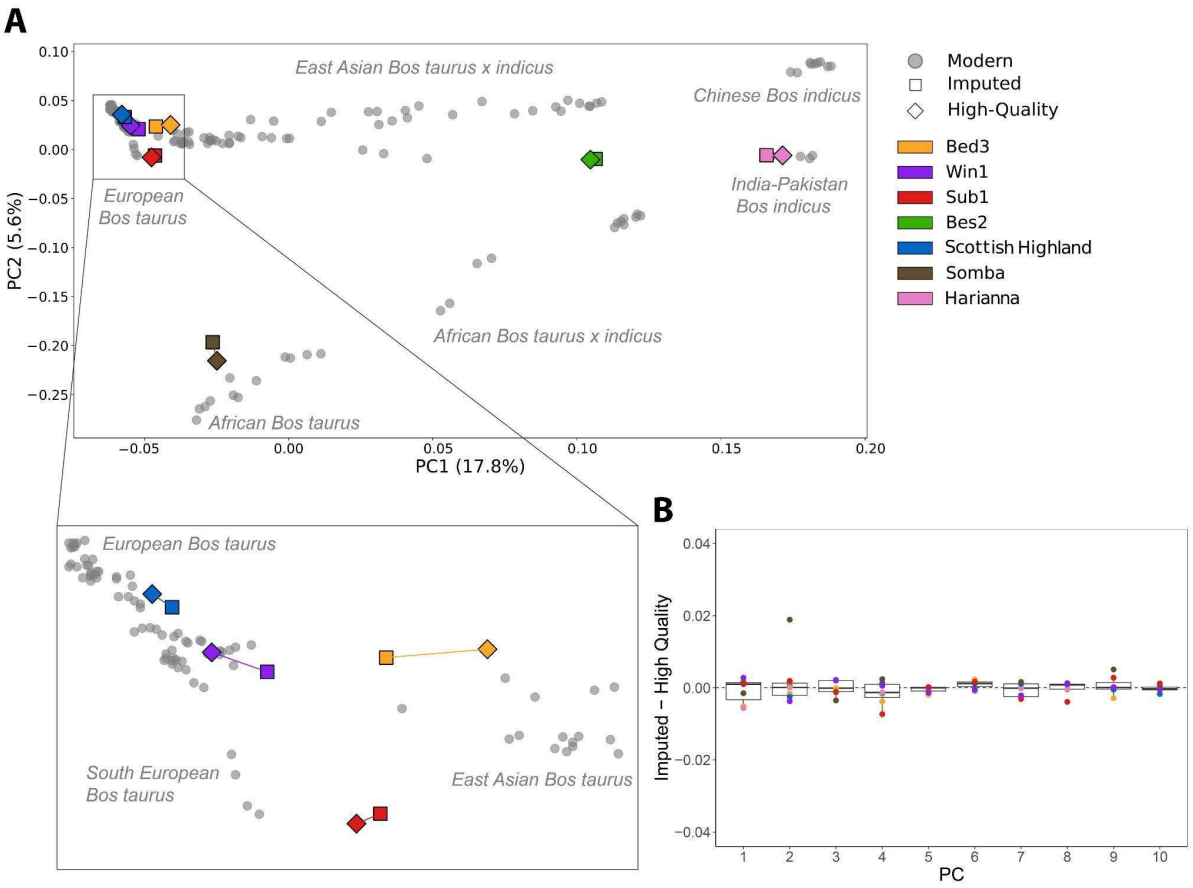

198

199 **Figure 3) Principal Components Analysis (PCA) of imputed and high-quality genotypes of the**
200 **seven test individuals onto the modern cattle reference panel A:** Projections for 0.5x imputed and
201 high quality diploid genotypes of the test samples onto the modern reference panel along the first two
202 eigenvectors. Dataset was filtered for a MAF ≥2.5%, transversions and LD pruning resulting in 812,801
203 SNPs. Test individuals are denoted by colour with imputed and high-quality represented by squares
204 and diamonds respectively, while the reference panel individuals are plotted as grey circles. **B:** Boxplots
205 of the normalised differences in the coordinates of the high-quality and 0.5x imputed genomes for the
206 first ten principle components. The horizontal lines of the box pot represent the first quartile, median
207 and third quartile, whiskers represent 1.5 times the quartile range.

208

209 For the first time we applied a runs of homozygosity (ROH) analysis on ancient cattle and
210 compared high-quality and imputed data (Figure 4; Figure SI 10). Patterns of ROH were
211 consistent when comparing the 0.5x downsampled imputation to the high-quality genotypes

212 (Figure 4; Figure SI 11). This was true for both genome-wide summaries of ROH (Figure 4A,
213 B) and in the detail of specific genome locations (Figure 4C; Figure SI 11). For example, a
214 large ROH of 15.8 Mb on chromosome 12 of the Mesolithic aurochs is identified using both
215 imputed and high-quality genotypes (Figure 4C; Figure SI 12).
216

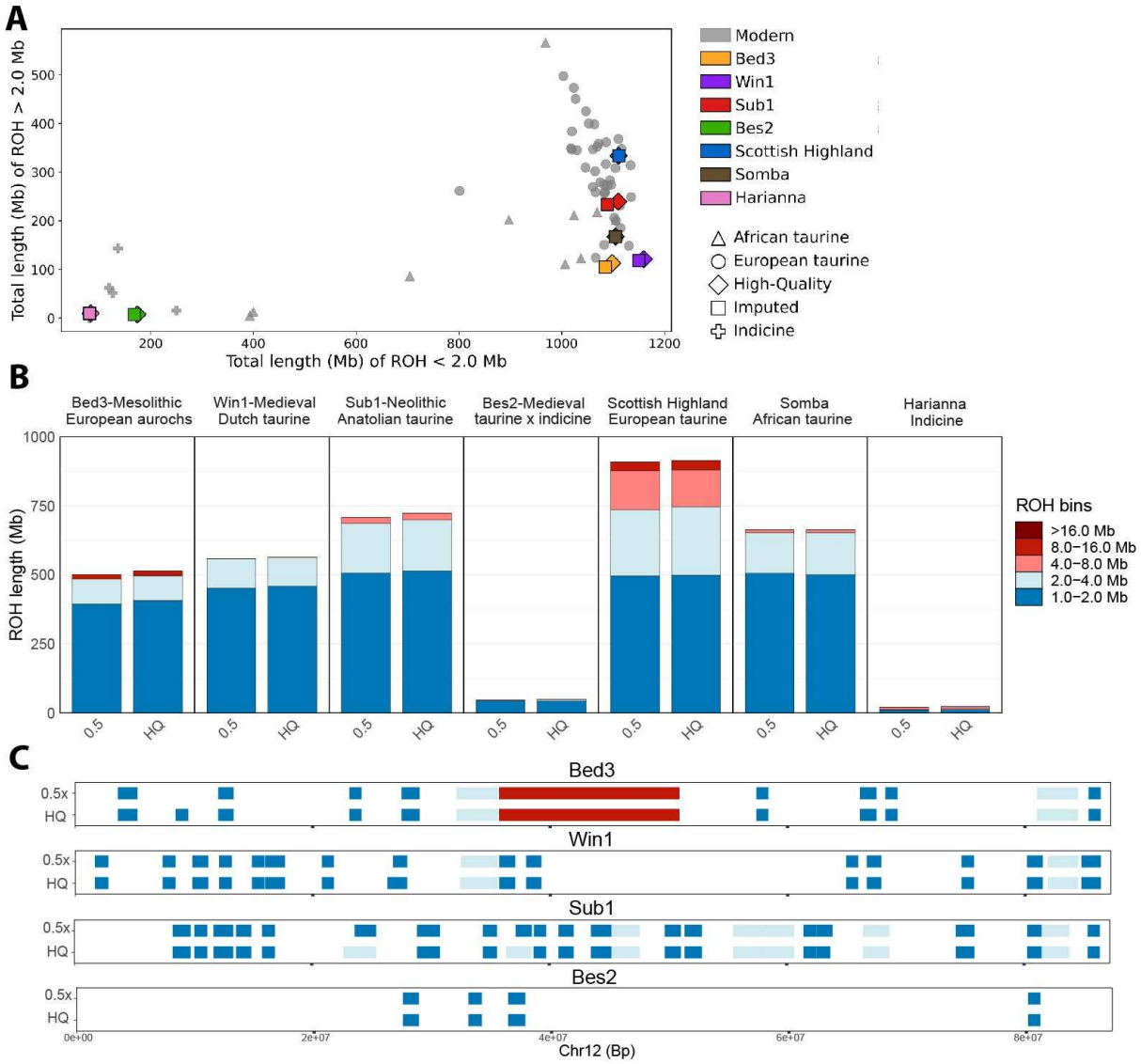

217

218 **Figure 4) Runs of Homozygosity (ROH) estimates for the 0.5x imputed and the high-quality**
219 **genotypes A**: The total length of ROH >2Mb and ROH ≤2Mb plotted with a subset of the reference
220 panel as a background in grey. Filtering included MAF ≥2.5%, transversions only and no missingness.
221 **B**: The total length of ROH split into length bins for the seven test samples. The number of sites used
222 for analysis = 481,786 filtered for a MAF ≥2.5%, transversions only and no missingness. **C:** Runs of

223 homozygosity along Chr12 for the four ancient genomes at 0.5x, and high-quality demonstrating the
224 general consistency between the imputed and high-quality dataset; filters are the same as B.
225
226 Moreover, imputation seems robust for estimating both recent genealogical and deeper
227 population histories via alternately small (<2 Mb) and large ROH (Figure 4A). In the test
228 samples the most pronounced inbreeding is in the modern Scottish highland sample; a feature
229 typical of European production breeds (Figure SI 10) (Purfield et al., 2012) and a pattern
230 absent from the ~1.5kyr Dutch sample. The ancient zebu hybrid, Bes2, had markedly low
231 levels of ROH, reflecting the large effective population size and genome diversity that is a well-
232 established feature of *Bos indicus* history (Bovine HapMap Consortium et al., 2009; Chen et
233 al., 2018; Murray et al., 2010).

234 We demonstrate that imputation of ancient cattle, including of the extinct European aurochs,
235 is a feasible methodology for future studies. The success of the imputation of aurochs implies
236 segregating haplotypes in the modern reference panel, most likely from introgression. While
237 damage is potentially disruptive, this is correctable with a deamination aware approach.
238 Imputation accuracy is high and is relatively consistent across the downsampled coverages,
239 demonstrating the feasibility of imputing ancient genomes as low as 0.5x or even lower. This
240 is demonstrated through the consistency in the analysis between imputed and high-quality
241 genotypes. The successful imputation of ancient cattle presents the opportunity for haplotype
242 aware analysis in the future.

243

244 **Materials and Methods**

245 **Ancient Processing - Bed3 & Win1**

246 The two archaeological samples were processed in dedicated ancient DNA laboratories in
247 Trinity College Dublin (Win1) and Johannes Gutenberg University of Mainz (Bed3).
248
249

Win1

A petrous bone, GIA collection number 3848, was excavated in 1997 from the site Winsum-Bruggeburen in the Netherlands. Site occupation was from 7th century BC to 14th century AD, and is thought to have been a military Roman outpost (Bos et al., 1997).

Sample preparation of Win1 was performed as described in (Verdugo et al., 2019). In brief, a wedge of bone was drilled and subsequently powdered using a mixer mill. DNA extraction of ~150mg bone powder followed a 48 hour 2-step double extraction of two 24 hour digestion steps (37°C) with fresh extraction buffer (0.5M EDTA pH8, 1 M Tris-HCl, 2% sodium dodecyl sulphate, and 100 µg/mL proteinase K) added after the first 24 hour period. Digestion was followed by a Tris-EDTA wash using Amicon® Ultra 4 mL filter (Merck Millipore) followed by a DNA purification step using the "QIAQuick minElute purification kit" (Qiagen) and eluted in 40 µL of EB buffer + Tween® 20 (Sigma-Aldrich) (Mattiangeli, 2023). Prior to library preparation a UDG-treatment was performed using 16.25ul of purified DNA and 5 µl (1U/1uL) USER enzyme (New England BioLabs®, Inc.) and an incubation of 3 hours at 37°C. Double stranded libraries were prepared (Meyer & Kircher, 2010) and sequenced (100 bp SE) on an Illumina Hiseq 2000 at Macrogen, Inc (1002, 254 Beotkkot-ro, Geumcheon-gu, Seoul, 153-781, Republic of Korea).

Radiocarbon dating was performed at 14CHRONO at Queen's University Belfast (UBA-29049 1556 ± 31 BP) and calibrated dates produced by OxCal 4.4 IntCal20 atmospheric curve (Ramsey, 2009; Reimer et al., 2020). (Figure SI 12)

Bed3

A petrous from an aurochs skull, find number 104/102-1, was excavated from the Mesolithic site of Bedburg-Königshoven in Germany (Street, 1999) along with numerous animal bones and two red deer skull headdresses (Wild et al., 2020). The site – today destroyed by lignite

277 mining – was a dump area, formerly located at the bank of a prehistoric wetland close to the
278 former river Erft (Street, 1999, 2020).
279
280 Sample preparation of Bed3 was performed as described for sample CTC in (Botigué et al.,
281 2017) and Ch22 and Th7 in (Verdugo et al., 2019), with the following alterations; two
282 independent extractions of 1g of bone powder were performed with a pre-lysis EDTA wash for
283 30 minutes at room temperature. Extracts underwent UDG-treatment and subsequently fifteen
284 double stranded sequencing libraries (Meyer & Kircher, 2010) were prepared and sequenced
285 (100 bp SE) on an Illumina Hiseq 2000 at Macrogen, Inc (1002, 254 Beotkkot-ro, Geumcheon-
286 gu, Seoul, 153-781, Republic of Korea) .
287
288 Radiocarbon dating was performed by CologneAMS at the University of Cologne in 2014 as
289 part of the Mesolithic project D4 of the CRC 806 (COL-2680-2.1 - 10036 ± 42) and calibrated
290 dates produced by OxCal 4.4 IntCal20 atmospheric curve (Ramsey, 2009; Reimer et al., 2020)
291 (Figure SI 13)
292
293 **Ancient Genome Alignment**
294 Fastq files were processed through a pipeline similar to (Verdugo et al., 2019). Reads were
295 trimmed for adapter sequences using cutadapt (v. 1.1) (Martin, 2011) (*-0 1 & -m 30*) and
296 aligned to ARS-UCD1.2 with the addition of the Y from BosTau5 using the Burrows-Wheeler
297 Alignment (v. 0.7.5a-r405) (Li & Durbin, 2009) with the sub-command aln (*-l 1024 -n 0.01 -o 2*).
298 BAM files were sorted with SAMtools (v. 1.9) (Li et al., 2009) and duplicates removed with
299 Picard (v. 2.20.3) (“Picard Toolkit,” 2019). Indel realignment was performed using the Genome
300 Analysis ToolKit (v. 3.3.0)(McKenna et al., 2010), SAMtools implemented for mapping quality
301 filtering (*-q25*) and coverage calculations performed by Qualimap (v. 2.1.3)(Okonechnikov et
302 al., 2015). To further minimise the effects of deamination, the soft clipping of five base pairs
303 at both ends of the reads was performed.
304

Modern Genome Processing

Publically available fastq files of 201 individuals (Table SI 6) were downloaded and processed through the following pipeline. Reads were trimmed for adapters using Trimmomatic (v 0.39) and aligned with BWA mem (v. 07.13)(Li, 2013). Reads were sorted and duplicates removed (PICARD 2.20.3)("Picard Toolkit," 2019) and properly paired reads retained (SAMtools v 1.9)(Li et al., 2009). Indel alignment was performed (GATK version v. 3.3.0)(McKenna et al., 2010) and reads filtered via samtools for mapping quality (q 25).

Variant Discovery

Variants (single nucleotide polymorphisms (SNPs) and insertions or deletions (INDELs)) were called from 201 mapped and filtered bam files of modern cattle (Table SI 6) with an average coverage above 7.6x using Graphtyper (Eggertsson et al., 2017), running each chromosome in parallel (Version 2.7.4). SNPs were removed if they were within 3bp of another INDEL or SNP with vcftools 0.1.17. INDELs were removed and SNPs were were filtered for bi-allelic alleles, a minimum genotype depth of 6x, a maximum genotype depth of 3 times the average genomic coverage of that individual, a minimum quality of 25 and a minimum genotype quality of 20 with vcftools version 0.1.17. SNPs were further filtered according to Graphtyper's guidelines with bcftools filter version 1.12 *(QD > 2.0, SB < 0.8, MQ > 40.0, LOGF > 0.5, AAScore > 0.5) (Li, 2011)*. As a final filtering step singletons, repetitive regions and genotypes with more than 20% missingness were removed with vcftools version 0.1.17 (Danecek et al., 2011), resulting in 21,656,053 high-quality SNPs, Table SI 2. After filtering, individuals with more than 20% missingness and individuals with 2nd degree relatives (>0.0885 score, vcftools relatedness2) were removed from the dataset resulting in 171 individuals (Table SI 2 & 6). The reference panel consists of 75 European *Bos taurus*, 27 Asian *Bos taurus*, 15 African *Bos taurus*, 10 African *Bos taurus x Bos indicus*, 5 southwest Asian *Bos taurus x Bos indicus*, 23 North East Asian *Bos taurus x Bos indicus* and 16 *Bos indicus*. The reference panel was phased using Beagle5 (Browning & Browning, 2007), with the parameters *impute=false, window=40, overlap=4, gp=true ne=20000*.

Pseudo-haploid Dataset

The previously published ancient low– to medium–coverage genomes (0.1-3.8x coverage range; Table SI 1) were pseudo-haploidized using ANGSD version 0.938 (Korneliussen et al., 2014) *doHaploCall*, with the following parameters: *doHaploCall 1*, *doCounts* 1, *dumpCounts* 1, minimum base quality of 30 (*-minQ 30*), minimum mapping quality of 25 (*-minMapQ 25*), retain only uniquely mapped reads (*-UniqueOnly 1*), remove reads flagged as bad (*-remove_bads*), remove triallelic sites (*-rmTriallelic 1e—4*), downscale mapping quality of reads with excessive mismatches (*-C 50*), discard 5 bases of both ends of the read (*-trim 5*), remove transitions (-rmTrans 1). The abovementioned sites in the modern reference panel (21,656,053 high-quality SNPs) were used as input for ANGSD using the parameter *–sites*. As a sanity check, the major/minor alleles of the low coverage ancient were compared to the modern reference panel and were removed if there were any discrepancies. ANGSD haplo files were transformed to plink tped files with the haploToPlink function from ANGSD version 0.938 and recoded into ped files with PLINK v.1.90 (Chang et al., 2015). Transitions were removed because transitions, unlike transversions, are most affected by postmortem deamination of DNA, which might increase the number of wrongly called SNPs. The restriction to transversions only is a standard approach in ancient DNA studies.

Genotype Imputation

Four ancient (13.8-18.7x coverage range) and three modern genomes (28.4-32.7x range) were downsampled to 0.25x, 0.5x, 1.0x and 2.0x on a chromosomal level using picard 2.20.0. The three high coverage (>28x) modern cattle were selected to represent European *Bos taurus* (Scottish Highland - ERR3305587), African *Bos taurus* (Somba - ERR3305591) and Indian *Bos indicus* (Harianna - SRS3120723). The downsampling was performed on chromosomal level so that average genomic coverage would not skew the downsampling process. Genotype likelihoods were computed for the downsampled and the original high-coverage genomes for the high-quality 21,656,053 SNPs mentioned in the Variant calling section.

Genotype calls and likelihoods were generated according to the GLIMPSE version 1.1.1 pipeline (Rubinacci et al., 2021), with the command bcftools mpileup (version 1.12) with parameters *-I ,-E, -a "FORMAT/DP,FORMAT/AD,INFO/AD"*, the reference genome and the abovementioned sites in the reference panel (*-T*) followed by bcftools call with the parameters *-Aim -C alleles*, and the abovementioned sites (*-T*). This step was performed on both downsampled and high-coverage genomes. The high-coverage genotype likelihoods were further filtered for a minimum base quality of 30, a minimum genotype quality of 25, a minimum genotype coverage of 8, a maximum genotype coverage of 3 times the average genomic coverage and a minimum allelic balance of 40%, obtaining the validation golden standard genotype likelihoods.

Imputation was performed on the downsampled genomes using GLIMPSE v1.1.1 (Rubinacci et al., 2021), according to the GLIMPSE pipeline. Chromosomes were split into chunks of 2 Mb with a 200kb buffer window with *GLIMPSE_chunk*. Imputation was performed on these chunks with default parameters using *GLIMPSE_phase* with the reference panel created in the section Variant calling. The imputed chunks were ligated using *GLIMPSE_ligate* with default parameters. The imputed data was filtered to keep only the most confidently imputed SNPs, this was done by filtering for a strict genotype probability *(GP) ≥0.99* and an *INFO score ≥0.99*, each sample was imputed and filtered separately. For imputation of the three modern test samples, reference panels without the test individual were created and subsequently used for imputation of the respective test sample.

Accuracy of Genotype Imputation

Imputation accuracy, seen as genotype concordance between the imputed and the high-quality validation genotypes, was calculated with Picard GenotypeConcordance version 2.20.0 ("Picard Toolkit," 2019). Imputation accuracy was calculated for heterozygotes, homozygotes alternative and the combined alternative alleles; this was done for eight MAF bins and a MAF threshold. Picards' GenotypeConcordance tool was used with the high-quality

validation genotypes as the *TRUTH_VCF*, the imputed genotypes as the *CALL_VCF*, and for the specific MAF bins mentioned previously with the *INTERVALS* parameter. Genotype concordance, called sensitivity in picards' output, is calculated as $TP\ /\ (TP\ +\ FN)$, where TP (true positives) stands for variants where the CALL matches the TRUTH, and FN (false negatives) stands for when variants do not match the reference. Recovery of genotypes is calculated as $(TP\ +\ FN)/\ Total\ HQ$, where Total HQ stands for the genotypes present in the high-quality validation TRUTH. Non-reference-discordance (NRD), a measurement of error rate was calculated following the formula published by (Sousa da Mota et al., 2023), NRD does not take correctly imputed homozygous reference sites into account, giving more weight to imputation errors at alternative sites.

Win1, an European taurine animal, demonstrates the lowest imputation accuracy of heterozygote and homozygote alternative alleles (Figure 2). While all ancient samples underwent UDG-treatment, deamination is still detected at CpG sites and in Win1 this is elevated throughout the first and last 30bp of the sequencing reads (Figure SI 2). We find that in this sample the imputation accuracy can be improved when we filter for potential deamination signals prior to imputation. This was achieved by a) setting heterozygote or homozygote reference genotypes as missing if the reference allele was T or A and the alternate C or G respectively b) setting heterozygote or homozygote reference genotypes as missing if the reference was T or A and the alternate allele was C or G respectively. Using these filtered genotypes we demonstrate an improvement in post imputation accuracy (Figure SI 3).

Downstream analyses

The filtered imputed and high-quality genotypes were merged with the modern reference panel using PLINK v.1.90 (Chang et al., 2015). In the case of PCA and admixture analyses, the data was filtered for MAF >2.5%, transversions only and linkage disequilibrium (indep-pairwise 50 5 0.5), resulting in 812,801 SNPs. For the ROH analysis, a subset of modern samples <5%

missingness (N=60) was created and merged with the imputed genotypes. The filters on the ROH dataset consisted of MAF >2.5%, no genotype missingness and transversions only, resulting in 481,786 SNPs.

PCA including ancient pseudo-haploid

The pseudo-haploid ancient samples were merged with the dataset containing the imputed and high-quality genotypes and modern reference panel, filtered for MAF >2.5%, transversions only and linkage disequilibrium (indep-pairwise 50 5 0.5), resulting in 812,801 SNPs. Smartpca version 16000 was used to perform a PCA with default parameters (Patterson et al., 2006; Price et al., 2006). The first 10 principal components were calculated using the modern reference panel, the pseudo-haploid, imputed and high-quality genotypes were projected (*lsqproject:yes)*.

PCA to test imputation genotypes

Smartpca version 16000 was used to perform a PCA with default parameters (Patterson et al., 2006; Price et al., 2006). The first 10 principal components were calculated using the modern reference panel, both the imputed and high-quality genotypes were projected (*lsqproject:yes)*. PCA was performed on each imputed coverage separately.

Model Based Admixture

ADMIXTURE v1.3.0 (Alexander et al., 2009) was used to estimate ancestry proportions for the modern reference panel, high-quality and imputed genotypes. ADMIXTURE ran for K between two and ten, for the best K's (4-5), a bootstrap with 1000 replicates (--B 1000) was run to obtain the standard error and bias of admixture estimates. Admixture ran on each imputed coverage separately.

Runs of Homozygosity (ROH)

ROH were estimated with PLINK v1.90 (Chang et al., 2015) with the parameters *--homozyg --homozyg-density 50 --homozyg-gap 100 --homozyg-kb 500 --homozyg-snp 50 --homozyg-window-het 1 --homozyg-window-snp 50 --homozyg-window-threshold 0.05*, according to earlier studies (Cassidy et al., 2016; Gamba et al., 2014; Martiniano et al., 2017; Sousa da Mota et al., 2023). ROH were estimated using a subset of moderns (<5% missingness), high-quality and imputed genotypes for each imputed coverage separately.

Data Availability

The raw reads for the two new ancient genomes will be deposited with ENA (Project XXXX). The accession numbers for the publicly available genomes used in the reference panel are noted in Table SI 1-2 & Table SI 6. The VCF of the phased reference panel will be made publicly available xxxx.

Acknowledgments

We are grateful to Daniel Bradley for his valuable mentorship, discussions and reading of the paper. We thank Daan Raemaekers, Canan Çakirlar, Joachim Burger and Conor Rossi for their reading of the paper and helpful suggestions. We thank GIA for access to the WIN1 sample. This work has been supported by The European Research Council under the European Union's Horizon 2020 research and innovation programme (885729-AncestralWeave, 295729-CodeX), Government of Ireland Postdoctoral Fellowship (GOIPD/2020/605) and Dutch Research Council Open Competition (Grant No. 406.18.HW.026).

References

Alexander, D. H., Novembre, J., & Lange, K. (2009). Fast model-based estimation of ancestry in unrelated individuals. *Genome Research*, *19*(9), 1655–1664.

Bos, J. M., Th. Niekus, M. J., Scheffer, J., & Volkers, T. B. (1997). OPGRAVING WINSUM-BRUGGEBUREN: ROMEINEN IN FRIESLAND! *Paleo-aktueel*, *9*, 65–69.

Botigué, L. R., Song, S., Scheu, A., Gopalan, S., Pendleton, A. L., Oetjens, M., Taravella, A. M., Seregély, T., Zeeb-Lanz, A., Arbogast, R.-M., Bobo, D., Daly, K., Unterländer, M., Burger, J., Kidd, J. M., & Veeramah, K. R. (2017). Ancient European dog genomes reveal continuity since the Early Neolithic. *Nature Communications*, *8*, 16082.

Bovine HapMap Consortium, Gibbs, R. A., Taylor, J. F., Van Tassell, C. P., Barendse, W., Eversole, K. A., Gill, C. A., Green, R. D., Hamernik, D. L., Kappes, S. M., Lien, S., Matukumalli, L. K., McEwan, J. C., Nazareth, L. V., Schnabel, R. D., Weinstock, G. M., Wheeler, D. A., Ajmone-Marsan, P., Boettcher, P. J., … Dodds, K. G. (2009). Genome-wide survey of SNP variation uncovers the genetic structure of cattle breeds. *Science*, *324*(5926), 528–532.

Browning, S. R., & Browning, B. L. (2007). Rapid and accurate haplotype phasing and missing-data inference for whole-genome association studies by use of localized haplotype clustering. *American Journal of Human Genetics*, *81*(5), 1084–1097.

Cassidy, L. M., Maoldúin, R. Ó., Kador, T., Lynch, A., Jones, C., Woodman, P. C., Murphy, E., Ramsey, G., Dowd, M., Noonan, A., Campbell, C., Jones, E. R., Mattiangeli, V., & Bradley, D. G. (2020). A dynastic elite in monumental Neolithic society. *Nature*, *582*(7812), 384–388.

Cassidy, L. M., Martiniano, R., Murphy, E. M., Teasdale, M. D., Mallory, J., Hartwell, B., & Bradley, D. G. (2016). Neolithic and Bronze Age migration to Ireland and establishment of the insular Atlantic genome. *Proceedings of the National Academy of Sciences of the United States of America*, *113*(2), 368–373.

Chang, C. C., Chow, C. C., Tellier, L. C., Vattikuti, S., Purcell, S. M., & Lee, J. J. (2015).

499 Second-generation PLINK: rising to the challenge of larger and richer datasets.
500 *GigaScience*, *4*, 7.
501 Chen, N., Cai, Y., Chen, Q., Li, R., Wang, K., Huang, Y., Hu, S., Huang, S., Zhang, H., Zheng,
502 Z., Song, W., Ma, Z., Ma, Y., Dang, R., Zhang, Z., Xu, L., Jia, Y., Liu, S., Yue, X., … Lei,
503 C. (2018). Whole-genome resequencing reveals world-wide ancestry and adaptive
504 introgression events of domesticated cattle in East Asia. *Nature Communications*, *9*(1),
505 2337.
506 Clemente, F., Unterländer, M., Dolgova, O., Amorim, C. E. G., Coroado-Santos, F.,
507 Neuenschwander, S., Ganiatsou, E., Cruz Dávalos, D. I., Anchieri, L., Michaud, F.,
508 Winkelbach, L., Blöcher, J., Arizmendi Cárdenas, Y. O., Sousa da Mota, B., Kalliga, E.,
509 Souleles, A., Kontopoulos, I., Karamitrou-Mentessidi, G., Philaniotou, O., …
510 Papageorgopoulou, C. (2021). The genomic history of the Aegean palatial civilizations.
511 *Cell*, *184*(10), 2565–2586.e21.
512 Daly, K. G., Maisano Delser, P., Mullin, V. E., Scheu, A., Mattiangeli, V., Teasdale, M. D.,
513 Hare, A. J., Burger, J., Verdugo, M. P., Collins, M. J., Kehati, R., Erek, C. M., Bar-Oz, G.,
514 Pompanon, F., Cumer, T., Çakırlar, C., Mohaseb, A. F., Decruyenaere, D., Davoudi, H.,
515 … Bradley, D. G. (2018). Ancient goat genomes reveal mosaic domestication in the Fertile
516 Crescent. *Science*, *361*(6397), 85–88.
517 Danecek, P., Auton, A., Abecasis, G., Albers, C. A., Banks, E., DePristo, M. A., Handsaker,
518 R. E., Lunter, G., Marth, G. T., Sherry, S. T., McVean, G., Durbin, R., & 1000 Genomes
519 Project Analysis Group. (2011). The variant call format and VCFtools. *Bioinformatics* ,
520 *27*(15), 2156–2158.
521 Eggertsson, H. P., Jonsson, H., Kristmundsdottir, S., Hjartarson, E., Kehr, B., Masson, G.,
522 Zink, F., Hjorleifsson, K. E., Jonasdottir, A., Jonasdottir, A., Jonsdottir, I., Gudbjartsson,
523 D. F., Melsted, P., Stefansson, K., & Halldorsson, B. V. (2017). Graphtyper enables
524 population-scale genotyping using pangenome graphs. *Nature Genetics*, *49*(11), 1654–
525 1660.
526 Erven, J. A. M., Çakirlar, C., Bradley, D. G., Raemaekers, D. C. M., & Madsen, O. (2022).

527 Imputation of Ancient Whole Genome Sus scrofa DNA Introduces Biases Toward Main
528 Population Components in the Reference Panel. *Frontiers in Genetics*, *13*, 872486.
529 Frantz, L. A. F., Haile, J., Lin, A. T., Scheu, A., Geörg, C., Benecke, N., Alexander, M.,
530 Linderholm, A., Mullin, V. E., Daly, K. G., Battista, V. M., Price, M., Gron, K. J., Alexandri,
531 P., Arbogast, R.-M., Arbuckle, B., Bălăşescu, A., Barnett, R., Bartosiewicz, L., … Larson,
532 G. (2019). Ancient pigs reveal a near-complete genomic turnover following their
533 introduction to Europe. *Proceedings of the National Academy of Sciences of the United*
534 *States of America*, 201901169.
535 Gamba, C., Jones, E. R., Teasdale, M. D., McLaughlin, R. L., Gonzalez-Fortes, G.,
536 Mattiangeli, V., Domboróczki, L., Kővári, I., Pap, I., Anders, A., Whittle, A., Dani, J.,
537 Raczky, P., Higham, T. F. G., Hofreiter, M., Bradley, D. G., & Pinhasi, R. (2014). Genome
538 flux and stasis in a five millennium transect of European prehistory. *Nature*
539 *Communications*, *5*, 5257.
540 Hayes, B. J., & Daetwyler, H. D. (2019). 1000 Bull Genomes Project to Map Simple and
541 Complex Genetic Traits in Cattle: Applications and Outcomes. *Annual Review of Animal*
542 *Biosciences*, *7*, 89–102.
543 Hui, R., D'Atanasio, E., Cassidy, L. M., Scheib, C. L., & Kivisild, T. (2020). Evaluating genotype
544 imputation pipeline for ultra-low coverage ancient genomes. *Scientific Reports*, *10*(1),
545 18542.
546 Korneliussen, T. S., Albrechtsen, A., & Nielsen, R. (2014). ANGSD: Analysis of Next
547 Generation Sequencing Data. *BMC Bioinformatics*, *15*, 356.
548 Librado, P., Khan, N., Fages, A., Kusliy, M. A., Suchan, T., Tonasso-Calvière, L., Schiavinato,
549 S., Alioglu, D., Fromentier, A., Perdereau, A., Aury, J.-M., Gaunitz, C., Chauvey, L.,
550 Seguin-Orlando, A., Der Sarkissian, C., Southon, J., Shapiro, B., Tishkin, A. A., Kovalev,
551 A. A., … Orlando, L. (2021). The origins and spread of domestic horses from the Western
552 Eurasian steppes. *Nature*, *598*(7882), 634–640.
553 Li, H. (2011). A statistical framework for SNP calling, mutation discovery, association mapping
554 and population genetical parameter estimation from sequencing data. *Bioinformatics* ,

27(21), 2987–2993.

Li, H. (2013). Aligning sequence reads, clone sequences and assembly contigs with BWA-MEM. In *arXiv [q-bio.GN]*. arXiv. http://arxiv.org/abs/1303.3997

Li, H., & Durbin, R. (2009). Fast and accurate short read alignment with Burrows–Wheeler transform. *Bioinformatics* , *25*(14), 1754–1760.

Li, H., Handsaker, B., Wysoker, A., Fennell, T., Ruan, J., Homer, N., Marth, G., Abecasis, G., Durbin, R., & 1000 Genome Project Data Processing Subgroup. (2009). The Sequence Alignment/Map format and SAMtools. *Bioinformatics* , *25*(16), 2078–2079.

Martiniano, R., Cassidy, L. M., Ó'Maoldúin, R., McLaughlin, R., Silva, N. M., Manco, L., Fidalgo, D., Pereira, T., Coelho, M. J., Serra, M., Burger, J., Parreira, R., Moran, E., Valera, A. C., Porfirio, E., Boaventura, R., Silva, A. M., & Bradley, D. G. (2017). The population genomics of archaeological transition in west Iberia: Investigation of ancient substructure using imputation and haplotype-based methods. *PLoS Genetics*, *13*(7), e1006852.

Martin, M. (2011). Cutadapt removes adapter sequences from high-throughput sequencing reads. *EMBnet.journal*, *17*(1), 10–12.

Mattiangeli, V. (2023). *Multi-step ancient DNA extraction protocol for bone and teeth v1*. https://doi.org/10.17504/protocols.io.6qpvr45b2gmk/v1

McKenna, A., Hanna, M., Banks, E., Sivachenko, A., Cibulskis, K., Kernytsky, A., Garimella, K., Altshuler, D., Gabriel, S., Daly, M., & DePristo, M. A. (2010). The Genome Analysis Toolkit: a MapReduce framework for analyzing next-generation DNA sequencing data. *Genome Research*, *20*(9), 1297–1303.

Meyer, M., & Kircher, M. (2010). Illumina sequencing library preparation for highly multiplexed target capture and sequencing. *Cold Spring Harbor Protocols*, *2010*(6), db.prot5448.

Murray, C., Huerta-Sanchez, E., Casey, F., & Bradley, D. G. (2010). Cattle demographic history modelled from autosomal sequence variation. *Philosophical Transactions of the Royal Society of London. Series B, Biological Sciences*, *365*(1552), 2531–2539.

Okonechnikov, K., Conesa, A., & García-Alcalde, F. (2015). Qualimap 2: advanced multi-

583 sample quality control for high-throughput sequencing data. *Bioinformatics* .
584 https://doi.org/10.1093/bioinformatics/btv566
585 Park, S. D. E., Magee, D. A., McGettigan, P. A., Teasdale, M. D., Edwards, C. J., Lohan, A.
586 J., Murphy, A., Braud, M., Donoghue, M. T., Liu, Y., Chamberlain, A. T., Rue-Albrecht, K.,
587 Schroeder, S., Spillane, C., Tai, S., Bradley, D. G., Sonstegard, T. S., Loftus, B. J., &
588 MacHugh, D. E. (2015). Genome sequencing of the extinct Eurasian wild aurochs, Bos
589 primigenius, illuminates the phylogeography and evolution of cattle. *Genome Biology*, *16*,
590 234.
591 Patel, A. K., & Meadow, R. H. (2017). South Asian contributions to animal domestication and
592 pastoralism. In U. Albarella, M. Rizzetto, H. Russ, K. Vickers, & S. Viner-Daniels (Eds.),
593 *The Oxford Handbook of Zooarchaeology* (pp. 280–303). Oxford University Press.
594 Patterson, N., Price, A. L., & Reich, D. (2006). Population structure and eigenanalysis. *PLoS*
595 *Genetics*, *2*(12), e190.
596 Picard toolkit. (2019). In *Broad Institute, GitHub repository*. Broad Institute.
597 https://broadinstitute.github.io/picard/
598 Price, A. L., Patterson, N. J., Plenge, R. M., Weinblatt, M. E., Shadick, N. A., & Reich, D.
599 (2006). Principal components analysis corrects for stratification in genome-wide
600 association studies. *Nature Genetics*, *38*(8), 904–909.
601 Purfield, D. C., Berry, D. P., McParland, S., & Bradley, D. G. (2012). Runs of homozygosity
602 and population history in cattle. *BMC Genetics*, *13*, 70.
603 Ramsey, C. B. (2009). Bayesian Analysis of Radiocarbon Dates. *Radiocarbon*, *51*(1), 337–
604 360.
605 Reimer, P. J., Austin, W. E. N., Bard, E., Bayliss, A., Blackwell, P. G., Ramsey, C. B., Butzin,
606 M., Cheng, H., Lawrence Edwards, R., Friedrich, M., Grootes, P. M., Guilderson, T. P.,
607 Hajdas, I., Heaton, T. J., Hogg, A. G., Hughen, K. A., Kromer, B., Manning, S. W.,
608 Muscheler, R., … Talamo, S. (2020). The IntCal20 Northern Hemisphere Radiocarbon
609 Age Calibration Curve (0–55 cal kBP). *Radiocarbon*, *62*(4), 725–757.
610 Rohland, N., Mallick, S., Mah, M., Maier, R., Patterson, N., & Reich, D. (2022). Three assays

611 for in-solution enrichment of ancient human DNA at more than a million SNPs. *Genome*
612 *Research*, *32*(11-12), 2068–2078.
613 Rubinacci, S., Ribeiro, D. M., Hofmeister, R. J., & Delaneau, O. (2021). Efficient phasing and
614 imputation of low-coverage sequencing data using large reference panels. *Nature*
615 *Genetics*, *53*(1), 120–126.
616 Sousa da Mota, B., Rubinacci, S., Cruz Dávalos, D. I., G Amorim, C. E., Sikora, M.,
617 Johannsen, N. N., Szmyt, M. H., Włodarczak, P., Szczepanek, A., Przybyła, M. M.,
618 Schroeder, H., Allentoft, M. E., Willerslev, E., Malaspinas, A.-S., & Delaneau, O. (2023).
619 Imputation of ancient human genomes. *Nature Communications*, *14*(1), 3660.
620 Street, M. (1999). Remains of Aurochs (Bos primigenius) from the Early Mesolithic site
621 Bedburg-Königshoven (Rhineland, Germany). In G.-C. Wenige (Ed.), *Archäologie und*
622 *Biologie des Auerochsen* (Vol. 1, pp. 173–194). Wissenschaftliche Schriften des
623 Neanderthal Museums.
624 Street, M. (2020). Sub-aquatic disposal of butchering waste at the early Mesolithic site of
625 Bedburg-Königshoven. In A, García-Moreno, H. Jm, S. Gm, L, Kindler, E. Turner, A,
626 Villalengua, & S, Gaudzinski-Windheuser (Eds.), *Human behavioural adaptations to*
627 *interglacial lakeshore environments* (Vol. 37, pp. 131–150). RGZM - Tagungen.
628 Verdugo, M. P., Mullin, V. E., Scheu, A., Mattiangeli, V., Daly, K. G., Delser, P. M., Hare, A.
629 J., Burger, J., Collins, M. J., Kehati, R., Hesse, P., Fulton, D., Sauer, E. W., Mohaseb, F.
630 A., Davoudi, H., Khazaeli, R., Lhuillier, J., Rapin, C., Ebrahimi, S., … Bradley, D. G.
631 (2019). Ancient cattle genomics, origins, and rapid turnover in the Fertile Crescent.
632 *Science*, *365*(6449), 173–176.
633 Vigne, J.-D., Gourichon, L., Helmer, D., Martin, L., & Peters, J. (2017). 84 The Beginning of
634 Animal Domestication and Husbandry in Southwest Asia. In Y. Enzel & O. Bar Yosef
635 (Eds.), *Quaternary in the Levant* (pp. 753–760). Cambridge Univ. Press.
636 Wild, M., Gehlen, B., & Street, M. (2020). Antler Headdresses. Implications from a many-
637 faceted study of an earliest Mesolithic phenomenon. *Quartär*, *67*, 205–223.